CrossMark

Design and Characterization of Bio-Chemical Sensor Based on Photonic Crystal Fiber with Fluorine-Doped Tin Oxides Film

Boyao Li[1,2] · Meng Wu[1,2] · Xinyu Liu[1,2] · Guiyao Zhou[1,2] · Teng Wang[1,2] · Zicheng Sheng[1,2] · Zhiyun Hou[1,2] · Changming Xia[1,2]

Abstract

The Mid-infrared waveband plays an important role in the biochemical sensing and material analysis, while the silica glass fiber is rarely used in the mid-infrared region due to the high transmission loss, and most of the silica glass fiber sensors are only used for testing refractive index. In order to achieve both of the concentration and functional groups of biological sample simultaneously, in this paper, we proposed a dual-channel integrated photonic crystal fiber sensor with fluorine-doped tin oxide (FTO) based on the unique optical properties of photonic crystal fibers and FTO. The surface plasmon polaritons (SPP) of FTO in the mid-infrared region has high sensitivity to the refractive index of surrounding material. Theoretical result shows that the confinement loss of the proposed fiber can be close to zero realized by a kind of unique super mode. Meanwhile, it also has a good structural error-tolerant rate, which reduces the difficulty of preparation. These findings have potential to apply the mid-IR waveband to detect multiple physical quantities simultaneously in the biochemical sensing field.

Keywords Photonic crystal fiber · Surface plasma · Super mode · Bio-sensor

Introduction

Sensing technology of photonic crystal fibers based on the surface plasmon polaritons has attracted lots of concerns in the last decade [1–7]. Among them, theoretically, the sensor proposed by Li et al. in 2015 based on surface plasma technology had reached the sensitivity of 12,450 nm/RIU for bio-chemical liquid [7]. Besides, Wu et al. fabricated a D-shaped fiber sensor in experiment. Its sensitivity is 21,700 nm/RIU [8]. However, the photonic crystal fibers in most reports were coated with Au or Ag that have plasma effect in visible or near-IR region, and they are almost only for detecting the refractive index of solutions [1–8]. In fact, for biochemical sensing, it should not only know the concentration of analytes but also its functional group, so as to acquire comprehensive understanding of the biological

sample. Many strong characteristic absorption peaks of functional groups in biochemical substances are mainly concentrated in mid-IR region; therefore, moving the working waveband of bio-chemical sensor to mid-IR is very important to improve detection sensitivity. Considering the material loss of silica glass is no more than 1000 dB/m [9] in mid-IR region, so we make it is 1 mm in length. Then, the material loss is no more than 1 dB. Besides, a kind of material whose plasma resonant frequency is in mid-IR waveband and short optical fiber length will be needed to reduce the loss of light.

Many doped semiconductors and other materials based on mid-IR plasmon polaritons have been reported, where transparent conductive oxides [10–15] are potentially useful SPP host materials such as indium tin oxide (ITO) [16] and FTO. Their carrier concentrations are lower than metal, so that the plasma resonance frequencies are in mid-IR or far-IR waveband. In practical applications, Javier Martínez et al. once used the surface plasmon polaritons of ITO in mid-IR to combine with conventional waveguide in order to propose a biochemical sensor. Owing to small carrier concentration of ITO in mid-IR, the sensitivity of the sensor which simply adopts the resonance of surface plasmon polaritons to test the sensitivity of sensors is not very good. What is more, it could only by analyzed the concentration of specified functional groups [17].

✉ Boyao Li
1943395872@qq.com

1   Guangzhou Key Laboratory for Special Fiber Photonic Devices, South China Normal University, Guangzhou 510006, China

2   Guangdong Provincial Engineering Technology Research Center for Microstructured Functional Fibers and Devices, South China Normal University, Guangzhou 510006, China

🙋 Springer

In order to improve the sensitivity of sensors with mid-IR plasmon polaritons and realize simultaneous detection of concentration and components, a kind of biochemical sensor doped with FTO, which is easier to doped than ITO, was proposed in this paper combining with the unique optical characteristics of photonic crystal fibers. The sensor has very good unique advantages: on the one hand, photonic crystal fibers are adopted to realize super mode transmission with low loss, different from works of Yang et al. [18] and Chou et al. [19], it utilizes the coupling function of core mode and SPP mode. It greatly improves the sensitivity of the sensor; on the other hand, concentration and components can be detected simultaneously. Besides, the temperature is also considered to explicit measurement in complex environment. Its high sensitivity of temperature can be used to calibrate the measurement result of analyte. To our knowledge, it is the first time that FTO combines with PCF, which is utilized for bio-chemical sensor that can detect multiple physical quantities simultaneously in mid-IR waveband. Its excellent performances are of great application value in the field of sensing.

Theories and Structure

In order to achieve the concentration and components of bio-chemical substance simultaneously, the sensor contains two integrated double channel (as shown in Fig. 1). For realizing the endless single mode and expediently testing the samples, the sensor embeds into the D-shaped PCF. For utilizing the SPP in the mid-IR, the FTO is coated on the D-shaped PCF. Then the light go through the polarizer; it will be divided into two beams. The one of the beams is on the FTO film, and it goes through the samples for analyzing the compositions of samples. Then, the signal can be collected in the channel 1. The other beams is in the core of D-shaped. Therefore, the signal can be tested in the channel 2 for detecting the concentrations utilizing the change of refractive index. So, the sensor

can realize the composition and concentration of analyte detect simultaneously.

In Fig. 2, the distance Λ between two adjacent air holes is 3 μm. In order to obtain fundament mode transmission and structural flexibility in photonic crystal fibers, the diameter dc of cladding air holes is selected as 0.49 Λ. The diameter of two small air holes above fiber core is expressed as d_1, and they serve to provide two big leakage channels in order to improve the sensitivity of core mode to the change of SPP mode, and t is the coating thickness of FTO.

The dispersion relation of pure silica glass can be obtained by Sellmeier equation [20], while the Drude free-electron model is adopted to get FTO [21]. For matching the practical consideration, the thickness of FTO in this paper is selected as 250 nm, and corresponding parameters of the Drude model have been given in ref. [22].

The confinement loss of guided mode can be represented as [23]:

$$L = \left| 8.686 \times \frac{2\pi}{\lambda} \mathrm{Im}(n_{\mathrm{eff}}) \times 10^4 \right| \tag{1}$$

where $\mathrm{Im}(n_{\mathrm{eff}})$ expresses the imaginary part of effective refractive index (dB/cm).

Results and Discussion

Sensing Properties

The paper used a full-vector finite-element-based modal solver to calculate the sensor above mentioned. Because the parameters of structure and material dispersion are given, we can study the sensor's optical properties in simulation tool. Considering the calculation accuracy and amount of calculation, the simulation model used in this work is 2D. Firstly, in order to detect the signal going through the sample in mid-IR,

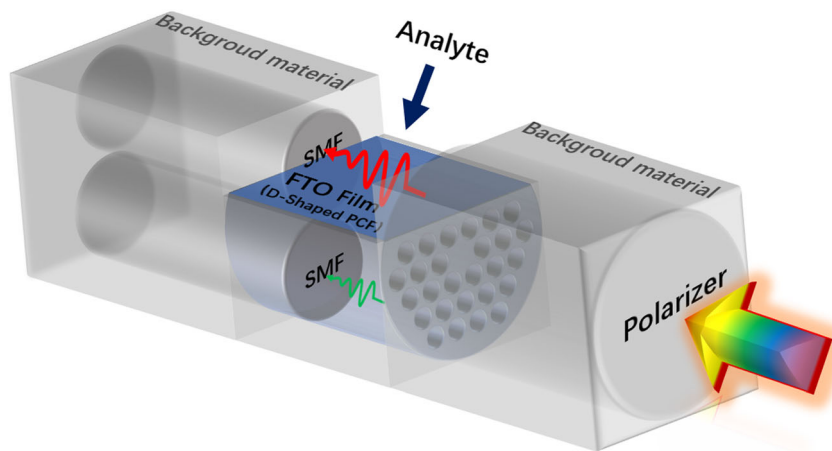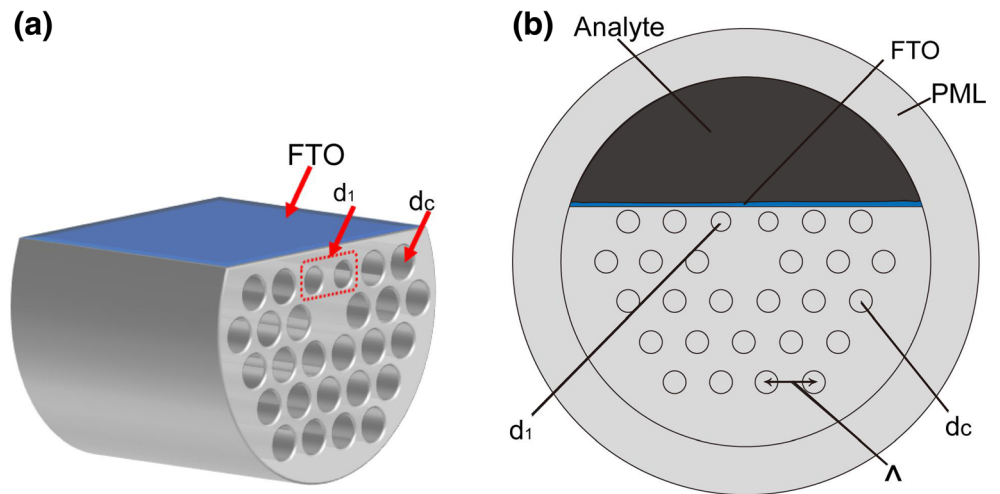**Fig. 1** The structural schematic diagram of the sensor

Fig. 2 The structure of D-shaped photonic crystal fibers coated with FTO. **a** The modal of D-shaped photonic crystal fibers. **b** Cross section of the modal in numerical simulation

we analyze the loss in the sample in the mid-IR (as shown in Fig. 3a) when the refractive index is 1.36. Obviously, the mode loss in mid-IR is low. So, the absorption signal of organic functional groups, such as imino group and hydroxyl and so on, can be collected in the spectrum, analyzed and cannot be lost. The signal can be easily collected. Next, we

consider the change of signal of refractive index. We calculate the loss of core mode in the D-shaped PCF. And the wavelength of the lowest confinement loss will change redshifted with decrease in the refractive index nf of the analyte (as shown in Fig. 3), but the minimum value of loss basically remains the same, which means that the sensitivity of the sensor is stable.

In order to study the cause of low loss in the sensitive band, we analyze the distribution of modal power. The following Fig. 4 shows that the distribution of modal power changes, and the core mode couples with SPP mode gradually with

increasing of wavelength in the same refractive index 1.36. At the point of low loss, the propagation mode is super mode jointly formed by three modes. In the waveband of high loss, the SPP mode, the mode in analyte, and core mode cannot interfere with each other to form a mutually bounded state, which results in energy leakage in the transmission process.

Further, study shows the imaginary part and confinement loss of super mode's effective refractive index when the analyte is 1.35, 1.355, and 1.36 (as shown in Fig. 5a, b). It can be seen clearly from Fig. 5a, with the increase of wavelength, the imaginary part of super mode's effective refractive index changes from positive value to negative one, and the confinement loss of optical fiber is 0 when the imaginary part of effective refractive index is 0. In addition, with the increase of the refractive index of analyte, blue shift occurs at 0 point of the imaginary part of super mode's refractive index, and then it also occurs at the lowest loss point.
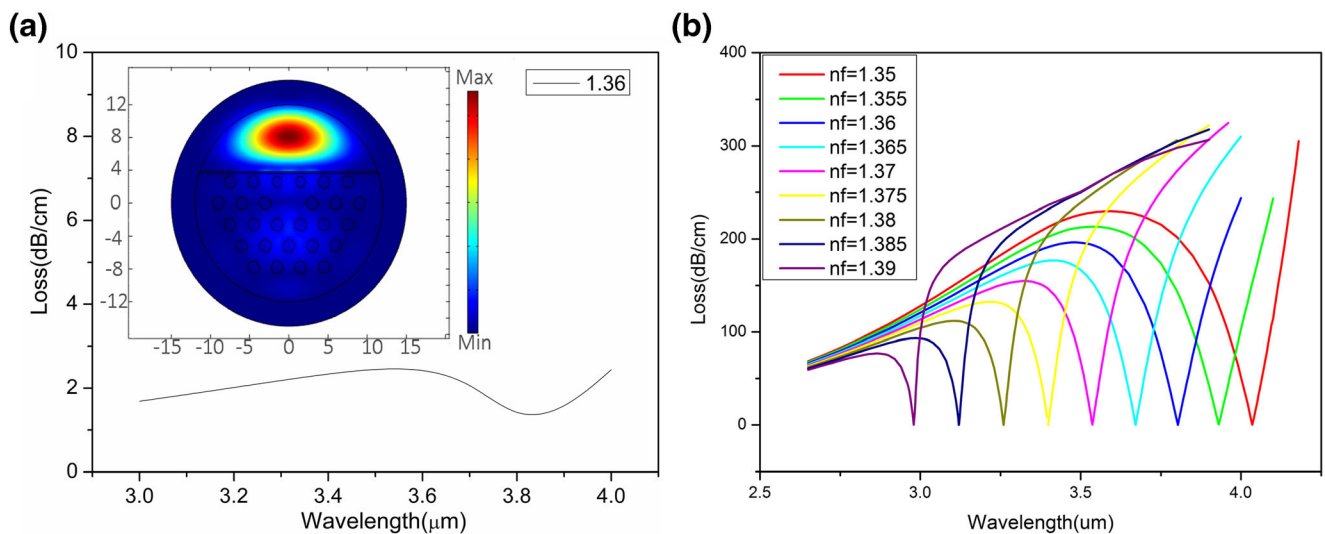
Fig. 3 The loss properties of different mode in the waveguide. **a** The mode loss in the analyte. **b** Changes of the loss valley with different analyte refractive index
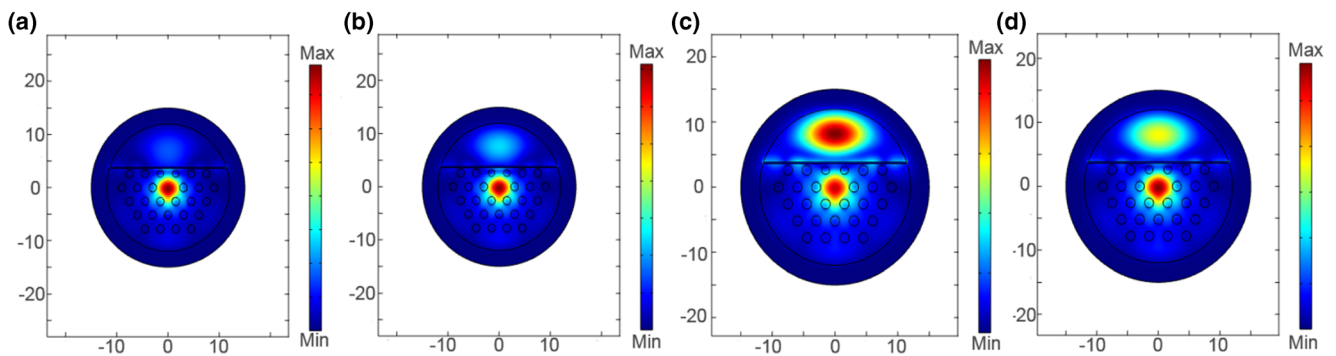
Fig. 4 The distribution of modal energy changes as the variation wavelength when analyte refractive index is 1.36. **a** loss = 181.66 dB/cm wavelength = 3.6 μm. **b** loss = 129.16 dB/cm wavelength = 3.7 μm. **c** loss = 0.717 dB/cm wavelength = 3.802 μm **d** loss = 145.47 wavelength = 3.9 μm

According to $S_\lambda(nmRIU^{-1}) = \Delta\lambda_{valley}/\Delta n_a$, the slope of sensitivity's fitting curve can be obtained (as shown in Fig. 6), which shows that the sensitivity of the sensor can reach 26,711.4 nm/RIU. The simulated values in 0 points with the increase of wavelength could be fitted with good linearity 0.99871. The minimum resolution of spectrometer is set to be 10 pm, so the resolution of the corresponding sensor is:

$$R = \Delta n \Delta\lambda_{min}/\Delta\lambda_{valley} = 3.7437 \times 10^{-7} RIU$$

Structural Characteristics

In the process of drawing photonic crystal fibers, the structure will inevitably change slightly. Here, we will discuss the influences of those structural parameters on sensing performance. In Fig. 7a, when the refractive index of the sample is 1.36, the lowest loss points occur red shift with the increase of pitch of holes Λ. However, the low loss of dip point keep 0, the responsivity of the sensor does not change. For the reason of occurring red shift, on the one hand, it can be explained from the aspect of wave optics. When assimilating the size of

objects can compare with optical wavelength, the diffraction of light is obvious. When the pitch of holes Λ increases, the coupling interference of evanescent field among modes moves towards longer waveband. On the other hand, it can be seen from Fig. 7b that red shift also occurs at 0 point of the imaginary part of super mode's refractive index when the pitch of holes Λ increases; therefore, the loss peak moves towards long wavelength.

Since d_1 locates between FTO layer and fiber core, its size will also affect the transmission stability of super mode in waveguides. Figure 7c shows that blue shift occurs at the loss valley of super mode with the increase of when the liquid to be tested is 1.36. But, the distance of shifts is little. The phenomenon can easily understand. Because the size of d_1 is less than wavelength, its subtle changes has little influence on the leakage of core mode. Besides, the loss valley value keeps to be 0; therefore, the sensitivity and responsivity of the sensor are hardly affected by d_1.

In the process of coating FTO on photonic crystal fibers, the thickness of FTO may not be very accurate as it is hard to
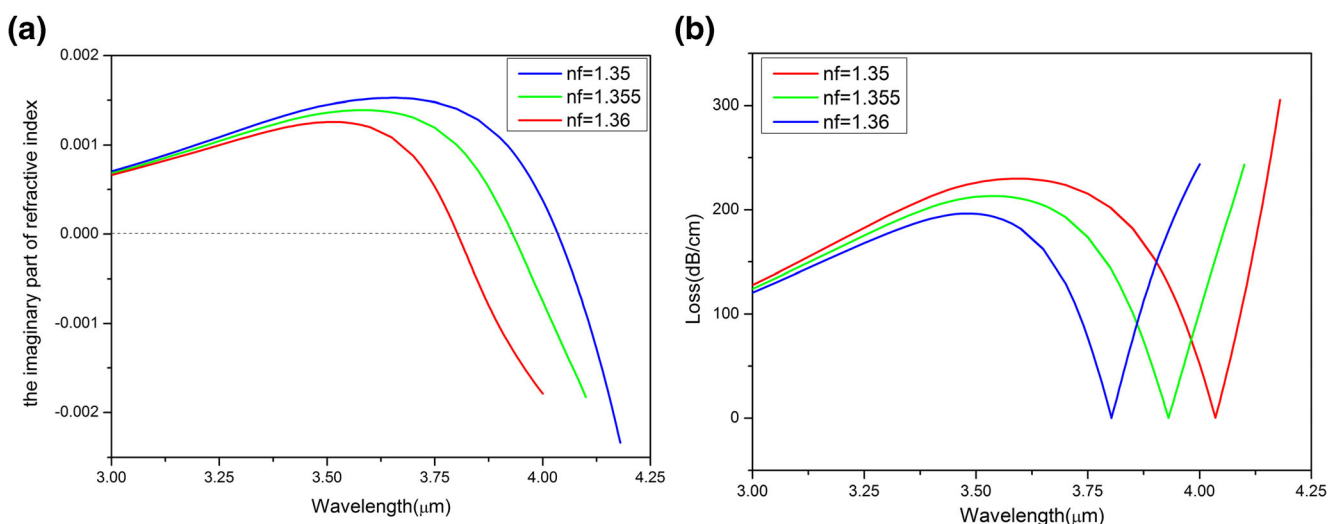

Fig. 5 The imaginary part of refractive index. The loss of core mode changes with the analyte's refractive index. **a** The imaginary part of refractive index occurs blue shift at 0 point with analyte refractive index increasing. **b** The loss valley occurs blue shift when analyte refractive index increasing
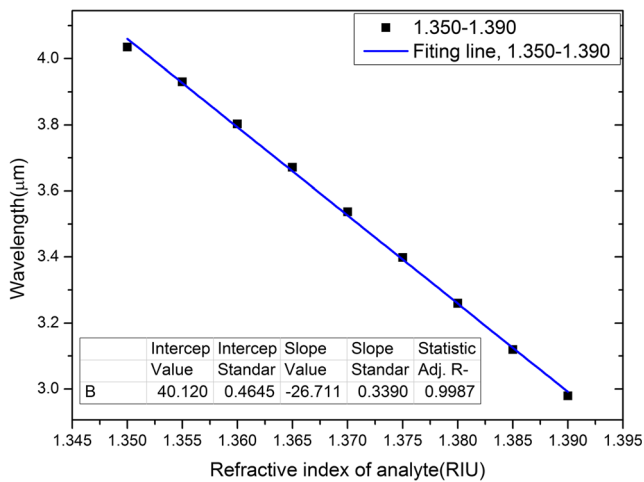
Fig. 6 The fitting line of sensitive wavelengths as a function of analyte refractive index

control. Figure 7d shows that there is almost no change for confinement loss with the change of thickness t when the refractive index of the sample is 1.36. As a kind of doped semiconductor, the carrier concentration of FTO is much lower than metal. The free electrons capturing photons rise with the increase of the thickness of FTO layer, but the magnitude is limited. Therefore, the thickness of FTO has little influence on the sensor's optical properties, and the shift of low loss is little.

Temperature Characteristics

In the process of practical application, the thickness of FTO changes slightly with the variation of temperature. Changes slightly with the variation of temperature. According to the analysis in the "Structural Characteristics" section, however, the change of FTO's thickness has little impact on loss valley. Due to low carrier concentration of FTO with the magnitude
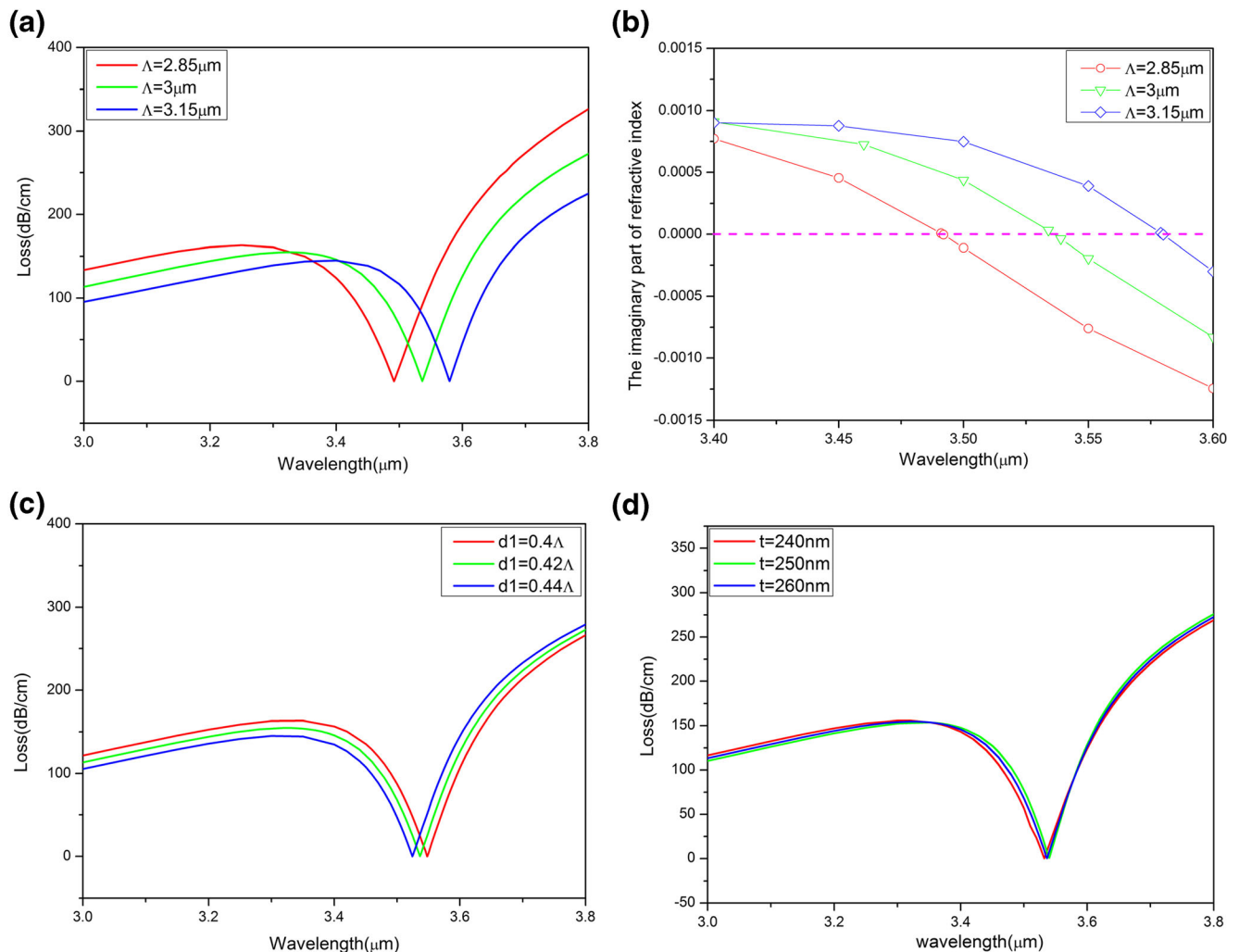

Fig. 7 The structure's influence on sensor's performance. **a** The confinement loss's changes with the variation of Λ. **b** The changes of the imagine part of refractive index with Λ. **c** The changes of valley loss corresponding to super-mode with variety of d_1. **d** The confinement loss's changes with the variation of t when sample's refractive index is 1.36.
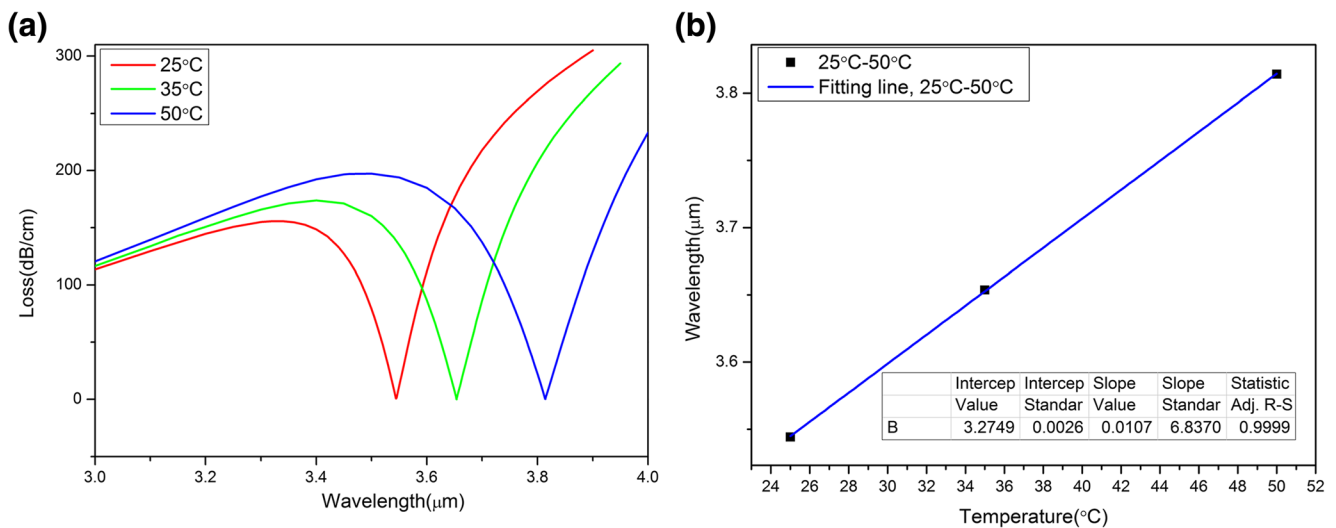
Fig. 8 The sensor's temperature performance. a The simulation results for the loss spectra of sensors with the temperature of 25, 35, and 50 °C. b The fitting line of sensitive wavelengths as a function of temperature

of $10^{20} \sim 10^{22} cm^3$, it is almost not affected by temperature. Compared with the change magnitude 10^{-4} of organic solvent's refractive index due to temperature, the effect of FTO's refractive index resulted by temperature can be ignored.

Considering that photonic crystal fibers are made by pure silicon, the dispersion relation of pure silica glass with the change of temperature has been given in literature [24] as follows:

$$n^2(\lambda, T) = (1.31552 + 0.690754 \times 10^{-5}T)$$
$$+ \frac{(0.788404 + 0.235835 \times 10^{-4}T)\lambda^2}{\lambda^2 - (0.0110199 + 0.584758 \times 10^{-6}T)}$$
$$+ \frac{(0.91316 + 0.548386 \times 10^{-6}T)\lambda^2}{\lambda^2 - 100}$$

where the unit of wavelength λ is micron and that of temperature T is Celsius. In addition, the thermal-optical coefficient $-4 \times 10^{-4}(°C^{-1})$ [25] of common organic solvent is selected as that of analyte.

According the change of material dispersion, we set parameter function in simulation tool. Then the change of sensor's optical characteristic can be calculated. Figure 8a shows the loss spectra of the sensor corresponding to temperature 25, 35, and 50 °C respectively when the refractive index of the analyte is 1.36. Apparently, the sensor is sensitive to temperature. The reason is super mode is common effects of the core mode and SPP mode. When the temperature changes, the material dispersion characteristic of whole structure also changes. Then, the optical properties of two mode changes. So, the sensitive point of super mode will change largely. Spectra detection is adopted, and the change of temperature can be detected through the wavelength shift of loss valley. The sensitivity of the corresponding sensor is:

$$S_\lambda(nm°C^{-1}) = \Delta\lambda_{valley}/\Delta T$$

In the above equation, ΔT represents the change of temperature, and the fitting result of the sensitive point is shown in Fig. 8b according to numerical calculation. The slope of fitting line is the sensitivity of the sensor, and it can be known from the figure that it is 10700pm/°C Assuming that the 10 pm position change of loss valley can be detected, the resolution of the sensor can reach to 9.3×10^{-4}°C. Therefore, the sensor can be used for biochemical sensing under a certain temperature and can also be used as a temperature sensor for a particular liquid.

Conclusion

The sensing properties of photonic crystal fiber combined with FTO are studied in this paper. Through adopting unique mid-IR SPP of FTO and flexible waveguide properties of photonic crystal fibers, the simultaneous measurement of concentration and components is realized for biochemical liquid. Because of special waveguide structure of photonic crystal fibers, the confinement loss of super mode can be close to 0 in sensitive waveband, which greatly improves signal-to-noise ratio. Finally, the sensitivity can reach as high as 26,711.4 nm/RIU, which is higher than the most existing reports. And it has very good linearity and error-tolerant rate of structure. In addition, it also has high sensitivity to temperature changes. The results show that the sensor has good application value in the field of biochemical sensor and also has a great application potential in the field of functional devices in mid-IR waveband through the combination of photonic crystal fibers and FTO.

References

1. Shuai B, Xia L, Zhang Y, Liu D (2012) A multi-core holey fiber based plasmonic sensor with large detection range and high linearity. Opt Express 20:5974–5986

2. Zhang Y, Zhou C, Xia L, Yu X, Liu D (2011) Wagon wheel fiber based multichannel plasmonic sensor. Opt Express 19:22863–22873

3. Zheng L, Zhang X, Ren X, Gao J et al (2011) Surface plasmon resonance sensors based on Ag-metalized nanolayer in microstructured optical fibers. Opt Laser Technol 43:960–964

4. Hunger D, Deutsch C, Barbour R, Warburton RJ, Reichel J (2012) Laser micro-fabrication of concave, low-roughness features in silica. AIP Adv 2:012119

5. Cennamo N, Massarotti D, Galatus R, Conte L, Zeni L (2013) Performance comparison of two sensors based on surface plasmon resonance in a plastic optical fiber. Sensors 13:721–735

6. Wang G, Li S, An G, Wang X, Zhao Y, Zhang W, Chen H (2016) Highly sensitive D-shaped photonic crystal fiber biological sensors based on surface plasmon resonance. Opt Quant Electron 48:46

7. Rifat AA, Ahmed R, Yetisen AK, Butt H, Sabouri A, Mahdiraji GA, Yun SH, Adikan FRM (2017) Photonic crystal fiber based plasmonic sensors. Sensors Actuators B Chem 243:311–325

8. Wu T, Shao Y, Wang Y, Cao S, Cao W, Zhang F, Liao C, He J, Huang Y, Hou M, Wang Y (2017) Surface plasmon resonance biosensor based on gold-coated side-polished hexagonal structure photonic crystal fiber. Opt Express 25:20313–20322

9. Humbach O, Fabian H, Grzesik U, Haken U, Heitmann W (1996) Analysis of OH absorption bands in synthetic silica. J Non-Cryst Solids 203:19–26

10. Shahzad M, Medhi G, Peale RE, Buchwald WR, Cleary JW, Soref R, Boreman GD, Edwards O (2011) Infrared surface plasmons on heavily doped silicon. J Appl Phys 110:123105

11. Soref R, Hendrickson J, Cleary JW (2012) Mid- to long-wavelength infrared plasmonic-photonics using heavily doped n-Ge/Ge and n-GeSn/GeSn heterostructures. Opt Express 20:3814–3824

12. Law S, Yu L, Wasserman D (2013) Epitaxial growth of engineered metals for mid-infrared plasmonics. J Vac Sci Technol Nanotechnol Microelectron Mater Process Meas Phenom 31:03C121

13. Boltasseva A (2014) Empowering plasmonics and metamaterials technology with new material platforms. MRS Bull 39:461–468

14. Noginov MA, Gu L, Livenere J, Zhu G, Pradhan A, Mundle R, Bahoura M, Barnakov YA, Podolskiy V (2011) Transparent conductive oxides: plasmonic materials for telecom wavelengths. Appl Phys Lett 99:021101

15. Franzen S, Rhodes C, Cerruti M, Gerber RW, Losego M, Maria JP, Aspnes DE (2009) Plasmonic phenomena in indium tin oxide and ITO-Au hybrid films. Opt Lett 34:2867–2869

16. Dominici L, Michelotti F, Brown TM, Reale A, Carlo AD (2009) Plasmon polaritons in the near infrared on fluorine doped tin oxide films. Opt Express 17:10155–10167

17. Martínez J, Ródenas A, Aguiló M, Fernandez T, Solis J, Díaz F (2016) Mid-infrared surface plasmon polariton chemical sensing on fiber-coupled ITO coated glass. Opt Lett 41:2493–2496

18. Yang KY, Chau YF, Huang YW, Yeh HY, Ping Tsai D (2011) Design of high birefringence and low confinement loss photonic crystal fibers with five rings hexagonal and octagonal symmetry air-holes in fiber cladding. J Appl Phys 109:093103

19. Chou Chau YF, Lim CM, Yoong VN, Syafi'ie Idris MN (2015) A simple structure of all circular-air-holes photonic crystal fiber for achieving high birefringence and low confinement loss[J]. J Appl Phys 118:243102

20. Agrawal GP (2007) Nonlinear fiber optics[M]. Academic press, San Diego

21. Wooten F (1972) Optical properties of solids[M]. Academic Press, Cambridge

22. Khalilzadeh-Rezaie F et al (2015) Fluorine-doped tin oxides for mid-infrared plasmonics. Opt Mater Express 5:2184–2192

23. Hasan MI, Abdur Razzak SM, Habib MS (2014) Design and characterization of highly Birefringent residual dispersion compensating photonic crystal Fiber. J Lightwave Technol 32:3976–3982

24. Ghosh G, Endo M, Iwasaki T (1994) Temperature-dependent Sellmeier coefficients and chromatic dispersions for some optical fiber glasses. J Lightwave Technol 12:1338–1342

25. Franco MAR, Serrão VA, Sircilli F (2007) Side-polished microstructured optical fiber for temperature sensor application. IEEE Photon Technol Lett 19:1738–1740